

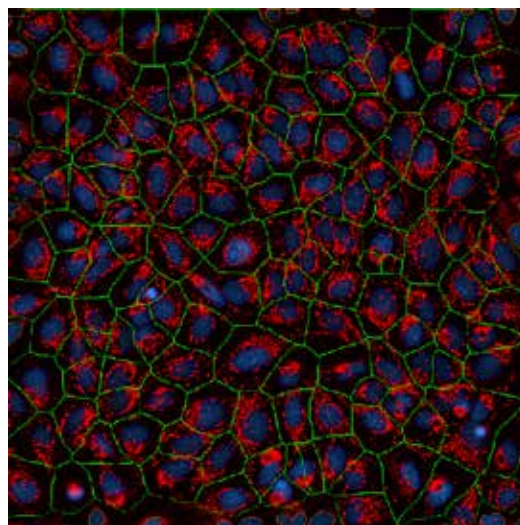
Phenotypic fingerprint of cellular function following gene editing by high-throughput imaging acquisition and analysis

Introduction

To effectively screen a large number of compounds or genes, high-throughput methodologies are essential. These can encompass either biochemical or cell-based assays. In order to assess spatial readouts—critical in interrogating relevant biological phenomena—fluorescence microscopy is required to increase throughput in order to handle the large sample numbers inherent in a genome-wide or small-molecule library screen. Automation of both image acquisition and analysis, commonly referred to as high-content analysis (HCA), achieves the desired throughput needs [1]. For this reason, HCA is routinely deployed in drug screening in the pharmaceutical industry [2]. High-throughput imaging-based assays have been applied to genome-wide screening where gene function has been disrupted either with siRNA [3] or CRISPR-Cas9 genome editing [4]. In this standard approach, a single assay parameter (for example, nuclear translocation, multiparameter cytotoxicity) is assessed as a function of each gene. In the following application note, we show an alternative approach using high-throughput imaging. Rather than using a single readout assessed across multiple genes, we pair the readouts from multiple cell-based assays following deletion of a signal gene. This provides a phenotypic “fingerprint” of cellular function in response to the loss of that particular gene. These fingerprints can serve as multiparametric readouts of potential off-target effects, as each of the cell-based readouts reflects an integrating node of cellular functions that will receive inputs from a plethora of signaling pathways. Alternatively, the fingerprint provided can be used as a template to overlay on responses within these assays following disruption of genes with unknown functions.

Genome editing

In the following application note, we describe the cellular consequences of CRISPR-Cas9-mediated deletion of *ATG5*. *ATG5* is a key gene involved in autophagy. *ATG5* forms part of the *ATG5-ATG12-ATG16* complex and is involved in the formation of autophagosome. Knockout (KO) models, both cell-based and animal, have shown that deletion of *ATG5* results in the loss of autophagosome formation and therefore attenuated autophagic capacity of these cells [5]. The loss of autophagosome formation is well characterized in *ATG5* KO cells, but what haven't been examined are the potential consequences on general cellular function. Following *ATG5* deletion in U2OS-Cas9 cells, we deployed a series of cellular assays to create a fingerprint of cellular responses occurring in response to disruption of autophagosome formation.



Proximal phenotypic assays

Autophagic and lysosomal assays that represent processes close to *ATG5* provide a picture of cellular events occurring similar to that in the gene of interest. They provide functional confirmation of the intended results that the gene deletion caused—in this case, loss of autophagosome formation, retarded autolysosome formation, and failure of cargo clearance (Figure 1). Loss of autophagosome formation results in reduced/no-cargo delivery to the lysosome. The impact of this perturbed cargo delivery was assessed using HCA and a suite of lysosomal probes. Using this approach, we were able to construct a fingerprint of lysosomal responses following perturbation of autophagy (Figure 2).

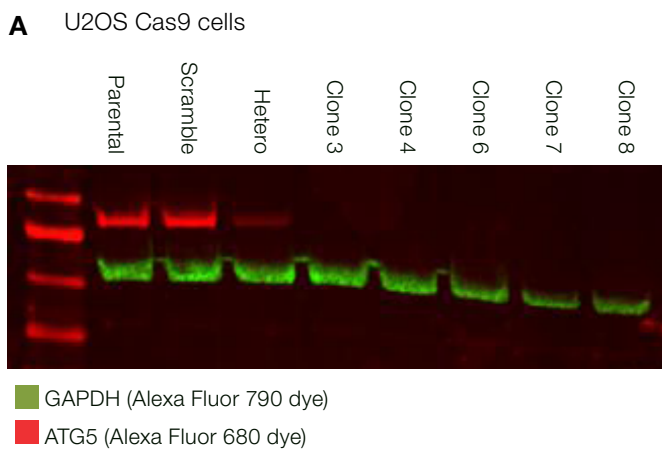


Figure 1. Data showing (A) functional confirmation of gene deletion effects by autophagic and lysosomal assays and (B) fingerprint of the disruption of macroautophagy.

Distal phenotypic assays

The effects of *ATG5* knockdown on processes closely related to autophagy provide a powerful analytical tool that describes a conserved set of cellular responses occurring upon inhibition of autophagosomal formation. Autophagy is a highly conserved pro-survival mechanism, and therefore perturbation of autophagy will impact numerous cellular processes. To measure the breadth of potential downstream targets affected by autophagy, we employed a series of cell-based assays and high-content imaging. Diverse processes such as proliferation, endocytosis, and protein synthesis can be assessed using fluorescent reporters. These data provided a holistic readout of cellular activity (Figure 3) serving to highlight cellular processes impacted by autophagy disruption.

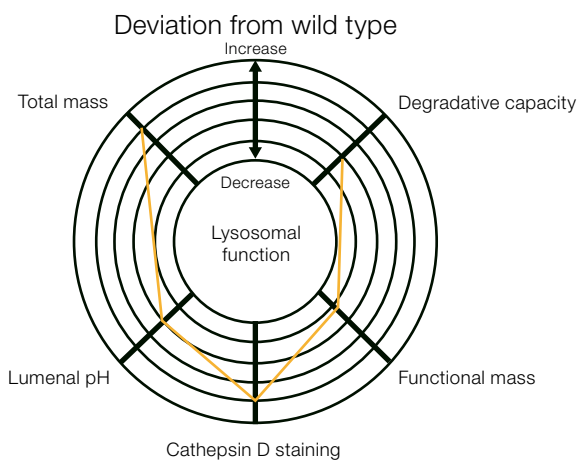
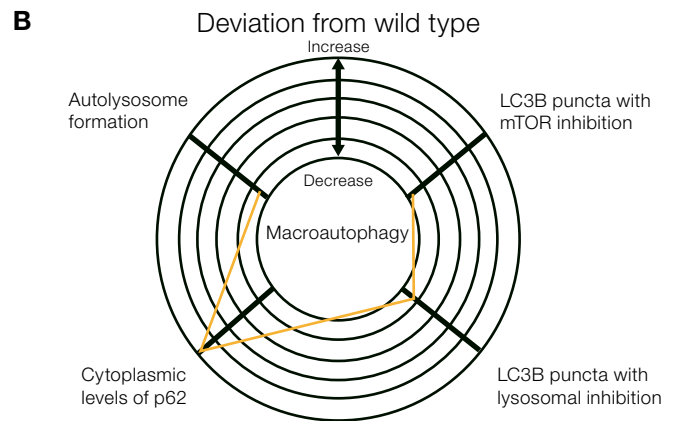


Figure 2. Fingerprint of lysosomal responses from autophagy perturbation.

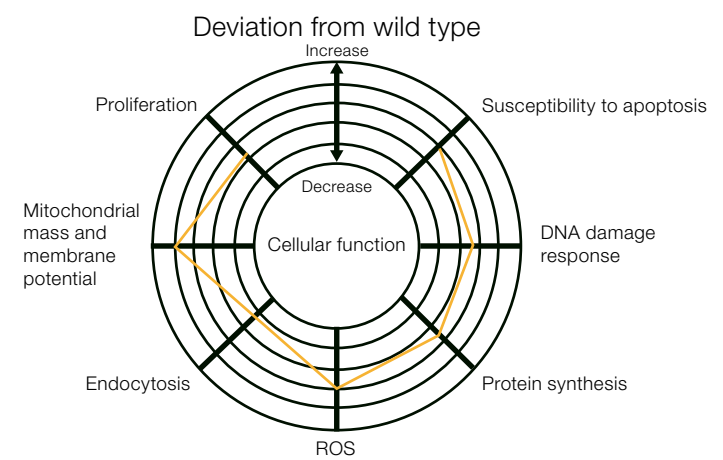


Figure 3. High-content imaging and analysis readouts featuring various cellular processes affected by autophagy perturbation.

Conclusions

The data shown outlines a powerful cell-based analytical approach. The cellular responses measured in *ATG5* KO cells provide insight into a broad number of processes potentially related to autophagy within cells. By examining a battery of cellular processes, one is able to detect potential off-target effects of targeted gene deletion or uncover hitherto unknown interplay between distal cellular pathways modulated by autophagy. Furthermore, by providing this multiparameter output, a fingerprint of cellular responses is created. This can be used as an overlay or signature of cellular responses that can be used to probe for other genes (or chemical modulators) producing an identical signature. This would indicate that the gene of unknown function, or compound, is acting in a similar manner to *ATG5*.

In this example, we have used autophagy as the cellular process and *ATG5* as the target gene, but the paradigm can be applied across other cellular processes and any gene. Therefore, this method represents a unique approach to uncovering novel gene function and the mode-of-action of novel small-molecule modulators. High-content imaging and analysis represents a powerful approach to gain this battery of responses. Not only can high-content imaging measure simple intensity-based readouts, similar to flow cytometry and plate readers, but it can also acquire spatial readouts. These spatial changes provide the most powerful and early indications of cellular signaling and functional disruption. Many critical cellular processes cannot currently be quantified using simple intensity-based readouts. This necessitates the implementation of imaging-based approaches. High-content imaging, by virtue of the automation of both image acquisition and analysis, provides the right sample size required to make statistically relevant measurements in a time frame that is suitable for experimental study. The ability to collect data from millions of cells within a single 96-well plate in a matter of minutes results in a thorough analysis performed over a reasonable length of time.

Materials and methods

Cell culture: U2OS cells stably expressing Cas9 were cultured in Gibco™ McCoy's 5A Medium supplemented with 10% FBS and 5 mg/mL blasticidin. Viability was recorded at each passage using an Invitrogen™ Countess™ II FL Automated Cell Counter (based on trypan blue exclusion).

Genome editing: To knock out genes in U2OS cells stably expressing Cas9, gRNA targeting *ATG5* (5 gRNAs targeting 3 exons) were designed using the Invitrogen™ GeneArt™ CRISPR Search and Design Tool ([thermofisher.com/crispr](https://www.thermofisher.com/crispr)). The gRNA was constructed using the Invitrogen™ GeneArt™ Precision gRNA Synthesis Kit and transfected into cells using the Invitrogen™ Neon™ Transfection System. Briefly, cells were transfected using 4 cycles of electroporation at 1,400 V for 15 ms. For *ATG5*, 4 µg of each gRNA was used when transfecting approximately 750,000 cells. Cell number was determined using the Countess II FL Automated Cell Counter to ensure accurate cell counts for transfection. Successful editing was confirmed by the genomic cleavage detection assay (GCD; data not shown) and by western blot analysis.

High-content imaging

Parental and *ATG5* KO U2OS Cas9 cells were plated at 5,000 cells/well and left overnight. Cells were counted at the time of plating using the Countess II cytometer to ensure consistent plating densities. Image acquisition was carried out on either a Thermo Scientific™ CellInsight™ CX5 or CX7 High Content Screening Platform using either a 10x (0.4 NA) or 20x (0.7 NA) air objective lens. Images were analyzed using Thermo Scientific™ HCS Studio 3 Cell Analysis Software using the following preset bio-applications. For autophagy, LC3B-positive puncta were identified with the autophagy bioapp. Colocalization of LAMP1 and LC3B was detected using the general colocalization measurement tool. All other lysosomal readouts were measured by the general spot measurement tool using Invitrogen™ LysoTracker™, LysoSensor™, LipidTox™, DQ™ Red BSA, and BODIPY™ FL Pepstatin A1 dye conjugates. Mitochondrial readouts were analyzed using a modified general spot detection algorithm using Invitrogen™ MitoTracker™ and Image-iT™ TMRM reagents. Assessment of apoptosis, DNA damage, and proliferation were quantified using the general intensity measurement tool. Translocation of NF-κB was assessed with a single translocation assay.

Western blot analysis of ATG5 protein

Cell pellets were prepared from parental cells and transfected with scrambled gRNA, and ATG5 hetero or 5 homozygous clones using Invitrogen™ Cell Extraction Buffer (Cat. No. FNN0011) and accompanying protocols. Additional reagents used in this study were: phenylmethylsulfonyl fluoride (PMSF) from Millipore Sigma and protease inhibitor cocktail (Roche). Each lane was loaded with 20 mg of protein. Equal loading was confirmed with anti-GAPDH antibody against U2OS cell lysate. Blots were imaged on the Invitrogen™ iBright™ Imaging System using Invitrogen™ secondary antibodies conjugated to Alexa Fluor™ dyes.

Cell labeling

All reagents were from Thermo Fisher Scientific unless stated otherwise. Reagents were used according to manufacturers' guidelines as follows:

- To measure proliferation, cells were incubated in 10 μ M of Invitrogen™ EdU for 30 minutes; the signal was detected with the Invitrogen™ Click-iT™ EdU proliferation kit using an azide-modified Alexa Fluor™ 488 dye.
- To measure mitochondrial membrane potential and mitochondrial mass, cells were loaded with Click-iT TMRM and MitoTracker Orange dyes at 100 nM for 30 min at 37°C in complete media. Cells were labeled with 1 μ M LysoSensor™ Green dye for 30 minutes at 37°C in complete media to measure lysosomal pH.
- To label lipid droplets, cells were fixed with 4% formaldehyde and labeled with a 1X solution of Invitrogen™ HCS LipidTOX™ Deep Red Neutral Lipid Stain and incubated for 30 minutes at room temperature in PBS.
- To measure endocytosis, cells were incubated with 250 μ g/mL of Invitrogen™ pHrodo™ Red dextran, 10,000 MW for 4 hours at 37°C in complete media.

- To label lysosomes, LysoTracker Red and LysoTracker Deep Red stains were loaded at 100 nM for 30 min at 37°C in complete medium.
- To label cathepsin, cells were labeled with 1 μ M BODIPY FL Pepstatin A for 1 hour at 37°C in complete media.
- To measure lysosomal degradative capacity, cells were incubated in the presence of 100 mg/mL DQ Red BSA for 2 hours in complete media. Following loading, cells were incubated for a further 3 hours in DQ Red BSA-free complete media.
- To assess viability, cells were labeled with Invitrogen™ Image-iT™ DEAD Green dye at 100 nM for 30 min at 37°C in complete media.

Primary antibodies

- Anti-LAMP1 (Cat. No. 15665) and anti-ATG5 (Cat. No. 12994S) antibodies, Cell Signaling Technology (CST)
- Anti-P62 (Cat. No. P0067), Millipore Sigma
- Invitrogen™ Anti-LC3B (Cat. No. L10382) and anti-GAPDH (Cat. No. 398600)

Detection antibodies

- Anti-LC3B was detected with a goat anti-rabbit secondary antibody conjugated to Alexa Fluor™ 488 dye.
- Anti-LAMP1 was detected with a goat anti-mouse secondary antibody conjugated to Alexa Fluor™ 647 dye.
- Anti-p62 was detected with a goat anti-rabbit secondary antibody conjugated to Alexa Fluor 488 dye.
- Anti-ATG5 and anti-GAPDH antibodies were detected with a goat anti-rabbit secondary antibody conjugated to Alexa Fluor™ 680 and a goat anti-mouse secondary antibody conjugated to Alexa Fluor™ 790 dyes, respectively, for western blot analysis.

References

1. Giuliano KA, Haskins JR, Taylor DL (2003) *Assay Drug Dev Technol* 4:565–577.
2. Moffat JG, Rudolph J, Bailey D (2014) *Nat Rev Drug Discov* 8:588–602.
3. Defrasnes C, Marsh GA, Foo CH et al. *PLoS Pathog* 12:e1005478.
4. Anderson EM, Haupt A, Schiel JA et al. (2015) *J Biotechnol* 211:56–65.
5. Kuma A, Hatano M, Matsui M et al. (2004) *Nature* 2004 432:1032–1036.

Find out more at thermofisher.com/detectcrispr

ThermoFisher
SCIENTIFIC